Electrokinetic remediation (EKR) effects under linear and radial electric field at laboratory scale

V. Pazzi[1], G.M.S. Losito[1], R. Mazzarelli[1], A. Trova[1], V. Lapenna[2] and E. Rizzo[2]

[1] DICeA, University of Florence, Italy

[2] IMAA-CNR Hydrogeosite Laboratory, Tito Scalo (Potenza), Italy

ABSTRACT   The remediation of polluted soils by heavy metals concerns wide areas of the planet, and the electrokinetic remediation (EKR) is an alternative method to the traditional ones. Moreover, in the current technologies this technique requests high power levels, with consequent security and cost problems. To enhance the process it is possible to use hydro-silica layers properties: these layers allow to move the heavy metals, if the electrical field is applied for a long time ($T > 24$ hours). Previous experiences showed that a sinusoidal waveform can improve the efficiency of the process up to 70%. In this paper we show the results of the EKR experiments carried out with two different electric fields: linear and radial. The electric field was controlled both as gradient and waveform (positive sinusoidal and DC). We worked with saturated sands polluted by Cr(VI). The process was monitored and calibrated using sets of voltage electrodes, chemical analysis and complex electrical resistivity of selected sand samples. The EKR process moved the 69% of Cr(VI) applying a linear electric field, while it moved the 34% of Cr(VI), applying a radial electric field. We also observed that the local electric resistivity is an efficient and economic index of the process, and the behaviour of the resistivity versus voltage let us presume that a positive ramp up signal, with a period of 12 hours, should be more effective than the positive sinusoidal one. Moreover, these experiments show that the process electrodeposits the heavy metal on to the surface of the high current electrode, consequently the polarity inversion of the applied electric field can clean this electrode and restore his "storage capacity".

1. Introduction

The heavy metal contamination is an international problem both for environment and human health: the remediation of polluted soils by heavy metals concerns wide areas of the planet.

The electrokinetic remediation (EKR) is an alternative method (Hamed *et al*., 1991; Acar and Alshawabkeh, 1993; Reddy *et al*., 2001; Virkutyte *et al*., 2002; Kim *et al*., 2009) to the traditional ones (soil washing, solidification/stabilization): it can be applied *in situ* and is one of the promising separation technologies and the most effective technique for fine-grained and/or clayey soil (Acar and Alshawabkeh, 1993).

The EKR process is due to the electrical migration and electroosmosis, together with the
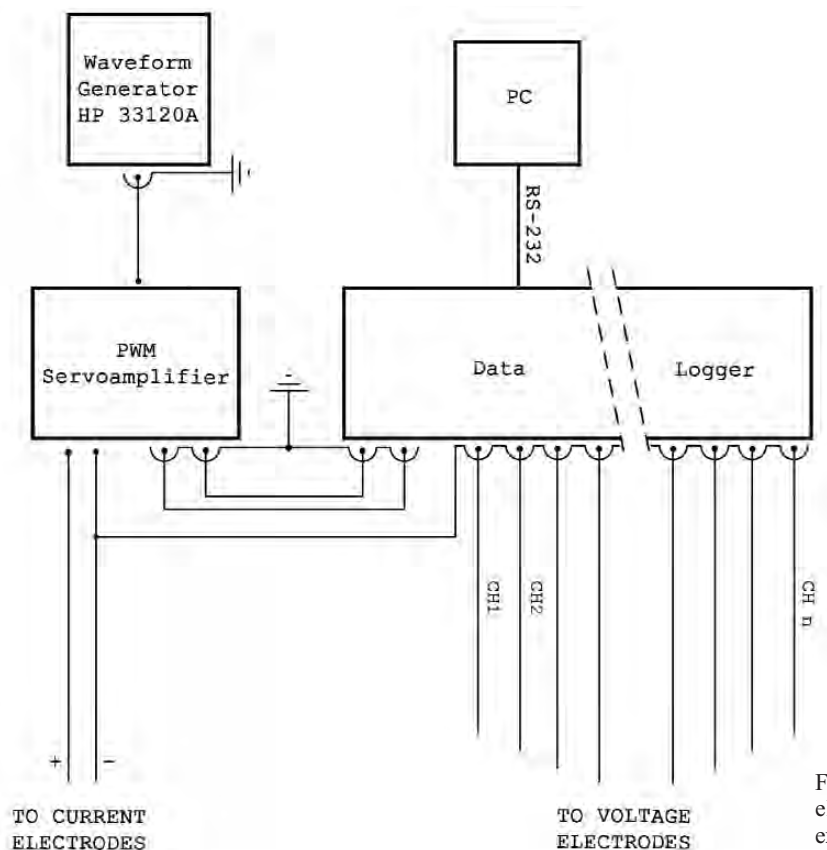
Fig. 1 - Block diagram of the electrical apparatus for EKR experiments.

electrolysis reactions at the electrodes. This technique uses direct current (order of 10 A/cm^2), or an electric voltage difference of some V/cm across electrodes placed in the ground. The groundwater is used as conductive medium and electrolysis reactions occur at the electrodes and produce O_2 at the anode and H_2 at the cathode. The chemical elements, that are diffused inside the pore fluid, will be moved by an electric field. This transport, together with sorption, precipitation and dissolution reactions is the fundamental mechanism affecting the EKR process.

The current technologies of the EKR request high power levels (some MW), with consequent security and cost problems (US Army Environmental Center, 2000).

Starting from 1998 at the Applied Geophysical Laboratory of the Florence University many experiments have been carried out to enhance the EKR: they have been developed on the basis of the previous experimental studies on electrical properties of hydrated clay rocks (Losito and Finzi-Contini, 1981; Losito *et al.*, 1991, 1995) and were aimed to find out an experimental procedure, that requests lower voltage levels (Losito *et al.*, 1998, 2001; Cherubini *et al.*, 2002; Losito and Angelini, 2002).

In particular, laboratory investigations and field measurements showed that the electrical behaviour of polluted soils is strongly non-linear at very low frequencies ($f < 0.01$ Hz). This phenomenon, typical of hydrated silicates, is enhanced by the heavy metal content (Losito and Angelini, 2002). In fact, at these frequencies, the electrical response of a water saturated porous
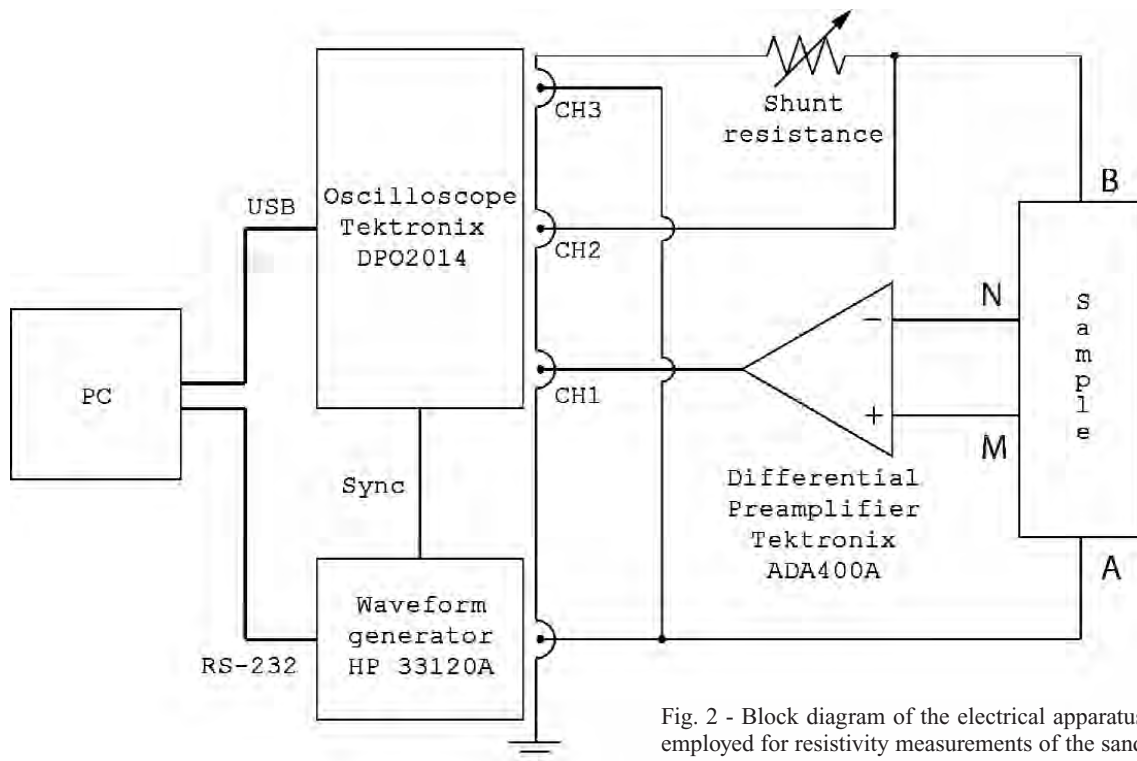
Fig. 2 - Block diagram of the electrical apparatus employed for resistivity measurements of the sand samples.

rock is sensitive to the properties of the mineral-water interface and to the polluted particles floating inside the fluid. This fluid/solid interaction produces non-linear electrical behaviour and consequently distortions of the electrical signals: if pure harmonic signals are used as applied voltage, the frequency content of the induced voltages is not monochromatic (Olhoeft, 1979).

Only if the Induced Polarization (IP) depends on linear phenomena, the frequency dispersion of the complex electrical resistivity ($\rho(\omega)$ [$\Omega \cdot$m]) can correctly describe the electrical polarization and the classical models can be used to interpret the electrical double layer (EDL) polarizations. The electrical characterization of the materials, that have a non-linear electrical behaviour, requests only a pure sinusoidal energizing waveform and must be defined by other parameters, in addition to the resistivity, like the Total Harmonic Distortion [THD: Olhoeft (1979), Losito *et al*. (1995)] and $V_{in} \Delta t$, that is a measure of the global electrical energy given to the material on Δt interval (Losito and Angelini, 2002).

The basic idea to enhance the EKR method was that the hydro-silica layers allow to move the heavy metals, if the electrical field is applied for a long time ($T > 24$ h) using a sinusoidal waveform (Losito *et al*., 1998; Losito and Angelini, 2002). In the previous EKR experiments, we selected the period of the sinusoidal energizing signal starting from the natural process period: this was evaluated applying for few days a DC signal to the metal polluted sand (Cherubini *et al*., 2002; Losito and Angelini, 2002). So doing, we obtained the 70% decontamination of the polluted sand at the end of the sinusoidal-EKR process.

The main purpose of the experiments presented in this paper is the evaluation of the influence

Table 1 - Physical parameters of the natural sands used for the EKR experiments: *v* (%) porosity and *d* (mm) grain diameter. Note that the Figline sand is lacking of the silt and clay components, while the Melfi sand is a very fine silica sand.

	v (%)	*d* (mm)								
		1024-5.66	5.66-2	2-1	1–0.5	0.50-0.25	0.250–0.125	0.125–0.063	0.063–0.032	< 0.032
Figline sand (%)	20-30	0.00	28.491	15.849	15.849	20.377	11.132	8.302	0.00	0.00
Melfi sand (%)	45-50	0.00	0.00	0.00	0.00	0.14	3.70	86.34	7.92	1.08

of different electrical field geometries on the decontamination levels: we selected a linear electrical field, used in the previous experiments (Cherubini *et al.*, 2002; Losito and Angelini, 2002) and a radial electrical field. Moreover, as heavy metal we selected Cr(VI), because it is widely used and is one of the most toxic elements; we studied different Cr(VI) concentrations and locations of the metal Cr(VI) solution: concentrated in a "bar" on the sand surface (see chapter 3) and diffused on the whole sand surface (see chapter 4).

2. EKR experiments

We carried out the EKR experiments to verify how the electrical field geometry acts on the Cr(VI) flux. In literature, there are not too many studies about the effects of electrode geometry on the removal efficiency of metals (Kim *et al.*, 2005; Turer and Genc, 2005; Zhang *et al.*, 2010). Moreover, we would verify if and how the monitored electrical parameters, and in particularly the resistivity ρ [$\Omega \cdot m$], may be employed to understand the EKR evolution, to avoid intermediate chemical analysis.

For the experiments we used an ad hoc electrical apparatus: Fig. 1 shows the block diagram of the apparatus used for the EKR process. The waveform generator (HP 33120A) and the data logger (AGILENT 34970A for DICeA apparatus and WK 6430B for IMAA-CNR one) are commercial products, while the PWM servoamplifier is a prototype made at the Applied Geophysical Laboratory of Florence. This instrument amplifies the generated waveform signal and allows to operate with *I* up to 2.5 A, *V* up to 400 V and arbitrary waveforms (DC – 1 kHz). The data logger channels were employed to obtain the induced voltage map of the cell surface.

Fig. 2 shows a block diagram of the electrical apparatus used for complex resistivity measurements of sand samples.

Table 2 - Chemical parameters of the natural sands used for the EKR experiments. Note the high content of CaO in the Figline sand and the relevant SiO_2 component in the Melfi of SiO_2.

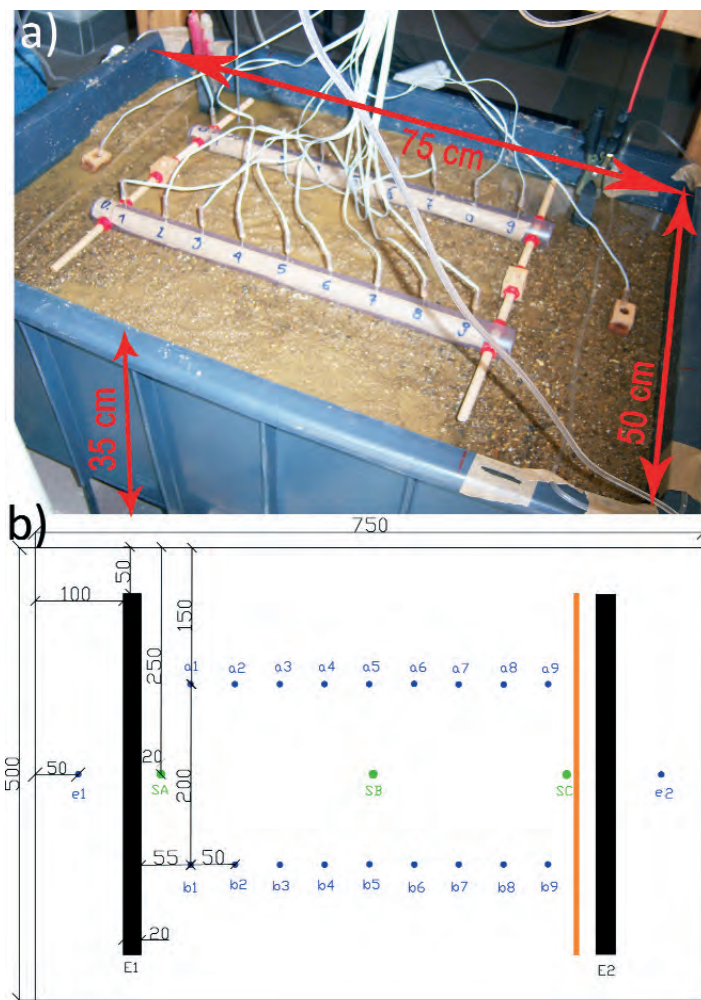|	SiO_2	Al_2O_3	Fe_2O_3	CaO	K_2O
Figline sand (%)	31.50	1.50	1.20	65.00	0.80
Melfi sand (%)	93.00	2.50	0.60	1.50	1.15

Fig. 3 - Photo (a) and CAD-layout (b) of the prismatic cell made at the Applied Geophysical Laboratory of the Florence University, Italy. In the layout dimensions are in mm; blue dots (sets a1-a9, b1-b9 and e1-e2) are the stainless-steel point voltage electrodes; black lines are the current line electrodes (E1-E2); orange line is the start Cr(VI) location; green dots (SA, SB and SC) are the log points for the sand chemical analysis.

2.1. Experimental methodology

To study the two electrical field geometries, the experiments were carried out at laboratory scale. We used two cells, that were respectively 100 times and nearly 1000 times bigger than those found in literature (Acar and Alshawabkeh, 1993; Baraud *et al.*, 1997; Reddy and Chinthamreddy, 1999; Kim *et al.*, 2005, 2009). We selected a prismatic cell, with a rectangular base, and a cylindrical cell, to study the pollutant transport, respectively due to a linear and to a radial electric field (Cherubini *et al.*, 2002; Turer and Genc, 2005).

To emphasize the effects on the material due to the linear and the radial EKR processes, we selected two different sands: the first one coming from Figline Valdarno (Florence, Italy) and the second one coming from Melfi (Potenza, Italy). The first sand was lacking of the silt and clay components (Table 1). As underlined in the introduction, these components are essential to active the electrophoresis process, one of the three migration movement that occur during the EKR (Losito and Angelini, 2002). The second sand was a very fine silica sand (SiO_2 93%, Table 2)
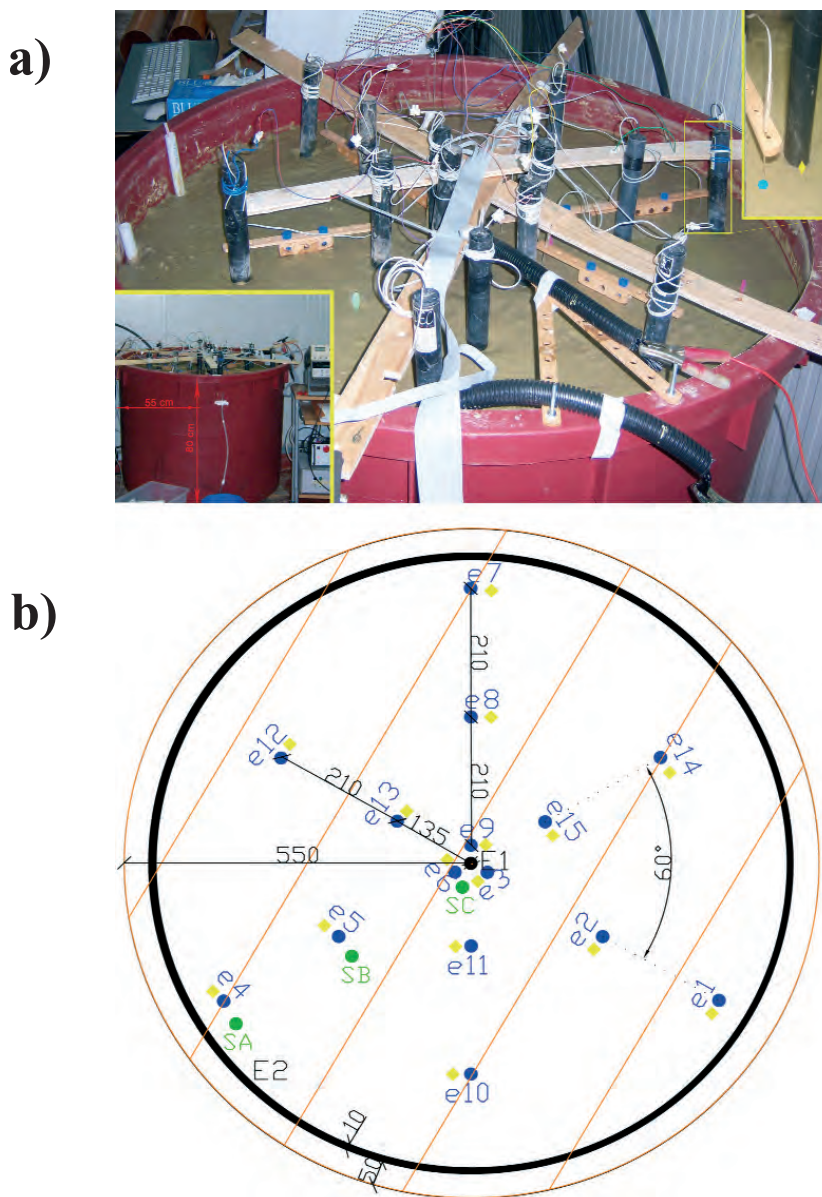
Fig. 4 - Photo (a) and layout (b) of the cylindrical cell made at IMAA-CNR of Potenza, Italy. In the layout: dimensions are in mm; blue dots (sets e1-e15) are the stainless-steel point voltage electrodes; yellow dots are the non-polarizable electrodes; black circle is the low current electrode (E2), while the black dot in the middle is the high one (E1); orange lines are the start Cr(VI) location; green dots (SA, SB and SC) are the log points for the chemical analysis.

useful to emphasize the pollutant behaviour under electric field.

As pollutant we selected the Cr(VI) as $Na_2CrO_4 \cdot 4H_2O$ (Losito and Angelini, 2002).

The EKR experiments were carried out using both constant and time-varying voltages at very low frequencies (quasi-DC: energizing period T = 24 h) (Cherubini *et al.*, 2002; Losito and
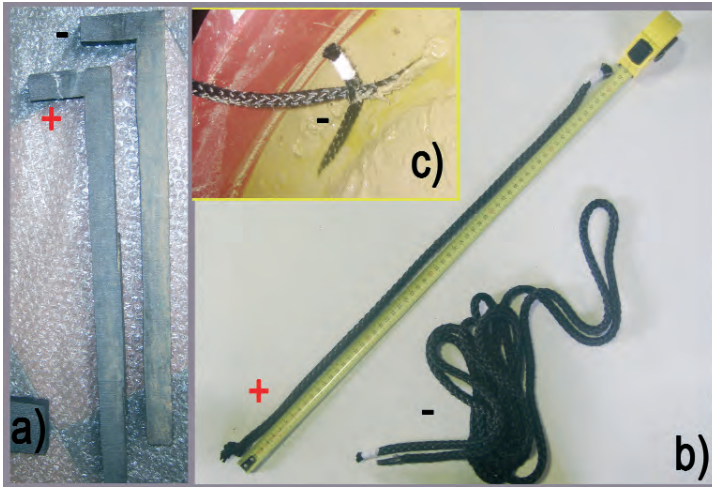
Fig. 5 - a) ®Sigrafrom HLM carbon bars by SGL Carbon Group (4 cm x 2 cm x 2.5 cm), employed as line current electrodes in the prismatic tank and b) the carbon-nylon ropes (Ø = 1 cm) by Pozzi Electa s.r.l., employed as current electrodes in the cylindrical cell.

Angelini, 2002).

To understand how the electrical resistivity parameter may be employed to evaluate the efficiency of the EKR process, we measured simultaneously, at 15 s sampling rate, the applied voltage V_{app} [V], the current I [mA] and the electric field on the sand surface (Figs. 1, 3, and 4). The spectral analysis of all signals showed that all the signal harmonic components had amplitude lower than 1% of the fundamental harmonic amplitude. Therefore we did not apply any numerical filter to the whole dataset. We calculated the resistivity only if the voltage and the current values were not too small ($I_{threshold}$ = 5 mA).

Giving the very low frequency of the applied voltage (T = 24 h) used in EKR process, the electrical resistivity of both the cells has been calculated using only the modulus (Parasnis, 1965) of the general complex apparent resistivity:

$$\rho_a = \left|\rho_a\right|e^{j\omega\Delta\varphi} = K\frac{\Delta Ve^{j\omega\Delta\varphi}}{I} \quad \left[\Omega\cdot m\right] \tag{1}$$

where: ρ_a is the apparent resistivity; $\Delta\varphi$ is the phase displacement between the input and the output signals; K [m] is the geometrical factor of the quadripole array; Δv [V] is the induced voltage and I[A] is the current.

The local resistivity (ρ_{ij} [$\Omega\cdot m$]) values of the experiments carried out with the linear electric field were calculated following the Telford's equation for a line-electrodes array (Telford *et al.*, 1976):

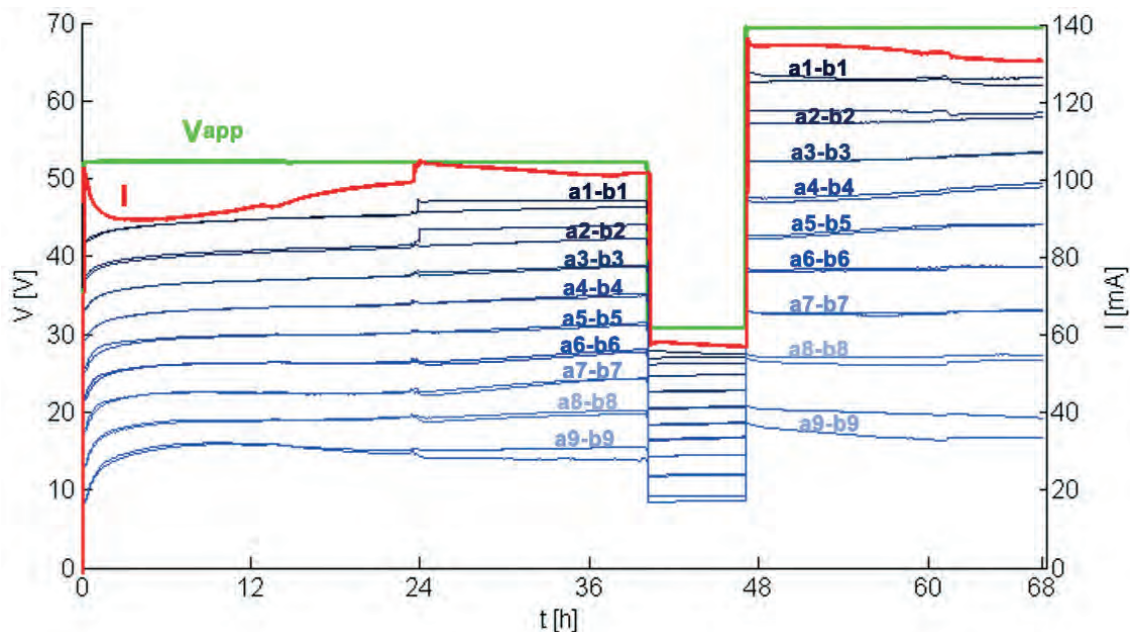$$\rho_{ij} = \frac{\pi}{4}\cdot\frac{V_{app}}{l_u}\cdot\frac{L^2 - x^2}{Ll} \quad \left[\Omega\cdot m\right] \tag{2}$$

Fig. 6 - Electrical signals (V_{app}, V_i and I) of the DC-EKR process with linear electric field. The tracking numbers are the electrode code (see Fig. 3 for the electrode codes).

where: V_{app} [V]: applied voltage; I_u [A/m]: current in the circuit for unit length of electrode; L[m]= $\overline{AB}/2$ (where $\overline{AB}$ is the distance between the current electrodes); l [m] = $\overline{MN}/2$ (where $\overline{MN}$ is the distance between the i and j voltage electrode); x[m]= $\overline{AM}+l$ (where $\overline{AM}$ is the distance between one of the current electrodes and the selected i voltage electrode).

In the experiments, the local resistivity of the prismatic cell was the resistivity of the sand volume having as thickness the distance between two consecutive voltage electrodes.

The local resistivity values of the experiments carried out with the radial electric field were obtained starting from the classical formula and consequently calculating the resistivity differences between two confining areas:

$$\rho_{ij} = 2\pi r_i \frac{v_i}{I_{tot}} \quad \left[\Omega \cdot m\right] \tag{3}$$

where: V_i [V] is the voltage at the i voltage electrode; I_{tot} [A] is the total current in the circuit; r_i [m] is the distance between i voltage electrode and the high voltage electrode (E1 in Fig. 4).

To calibrate the local resistivity by means of chemical analysis of Cr content, we logged the sand near the two current electrodes and halfway between them, at the beginning and at the end of each energization process. These sampling locations are indicated by green letters (SA, SB, SC) in Figs. 3 and 4.
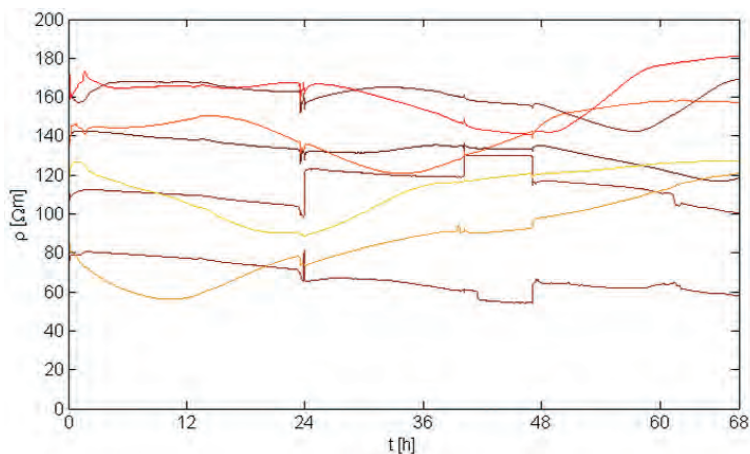
Fig. 7 - Local electrical resistivity ρ_{ij} versus time, during the DC-EKR linear process. The ρ_{ij} were calculated by means of the Telford's equation for a line-electrodes array (see chapter 2.1). See Fig. 9 for the chromatic scale.

The sand samples were analyzed by the atomic absorption method at the Microanalysis Laboratory of the Department of Organic Chemistry of the Florence University, according to the D.M. September 13, 1999 of the Italian Ministry of Agricultural and Forestry Policy.

Moreover, to calibrate the electrical resistivity variations occurred during the EKR processes, we measured the complex electrical resistivity following the experimental method described before (Losito *et al.*, 1995, 1998; Losito and Angelini, 2002).

3. Linear electric field experiments

3.1. Experimental setup

The prismatic cell with a rectangular base (50 cm x 75 cm, high: 35 cm) was made of a non-polarizable plastic material (Fig. 3a). It was filled to a depth of 30 cm with natural sand coming from Figline Valdarno (sand volume ≈ 130 dm^3). The granulometric parameters of this sand are shown in Table 1. The sand was saturated with 23 dm^3 of tap water and a piezometer was used to take under control the saturation.

The current electrodes were two Sigrafrom® HLM carbon bars by SGL Carbon Group (4 cm

Table 3 - Cr_{tot} content [mg/kg$_{dry\ soil}$] detected by the atomic absorption method, according to the D.M. September 13, 1999 of the Italian Ministry of Agricultural and Forestry Policy, during the three EKR chained processes (DC, SIN and SIN-INV) carried out with two line current electrodes (see chapter 3). The location of the sand samples is indicated in Fig. 3.

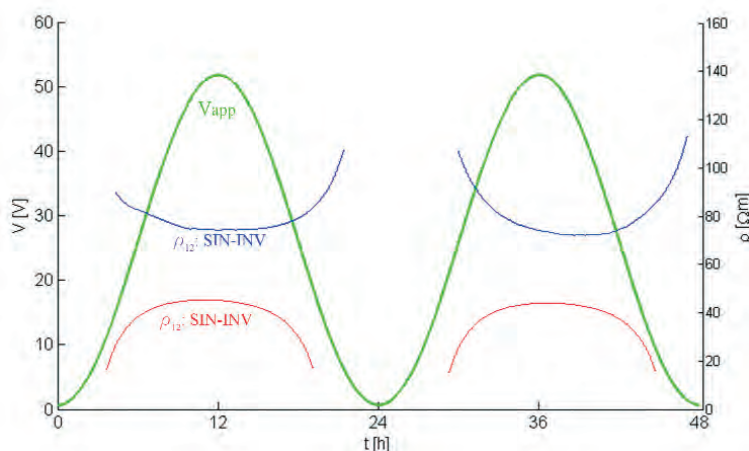| ID Sample	Cr_{tot} content [mg/kg$_{dry\ soil}$]			
	24 h DC	68 h DC	48 h SIN	48 h SIN-INV
SA	32.22	50.50	65.45	50.30
SB	40.00	31.81	32.60	34.83
SC	38.53	39.82	32.64	31.62

Fig. 8 - Local resistivity ρ_{12} versus time, during the SIN process (red lines) and the SIN-INV process (blue lines), calculated in reliable intervals. The trend inversion of the "blue lines" is a marker of the ion flux. The green line is the applied voltage V_{app}.

x 2 cm x 2.5 cm) (Fig. 5a). They were L-shaped: the longer side of the bars was located 1 cm depth , the L-side shorter was outcropping and used for the electrical connections (Fig. 3a).

The current electrodes were 51 cm spaced and located 10 cm away from the shorter side walls of the tank, and 5 cm away from the longest side walls (Fig. 3b).

Eighteen stainless steel voltage electrodes ($\varnothing = 0.2$ cm, $L = 5$ cm) were placed 1 cm depth within the current electrodes, to monitor the local electrical voltage. They were located on two parallel rows, 5 cm steps; the distance between the two rows were 20 cm (a1-a9, b1-b9 in Fig. 3b). More, two voltage electrodes (e1-e2 in Fig. 3b) were placed outside the line current electrodes to indirectly control the Cr flux outside the current electrode. The twenty voltage electrodes were connected to the data logger by means of unipolar cables (the light gray cable in Fig. 3a). In particular given the very low-frequency electrical field, the shields are not necessary.

We polluted the sand with 10 cm^3 of a 0.36 g Cr(VI) solution. This solution was injected ^{3}cm far from the low voltage electrode (orange line near E2, Fig. 3b), into a "channel" placed at 2 cm. The starting sand polluted volume was about 6 dm^3.

After the tank was arranged, the current electrodes were short-circuited and the system send-

Table 4 - Complex electrical resistivity $\rho\,(\omega)$ [Ωm] of one natural Melfi sand sample and four polluted sand samples at very high frequency ($f \approx 15$ kHz) using two-electrode technique (see chapter 5). The location of the sand samples is indicated in Fig. 4.

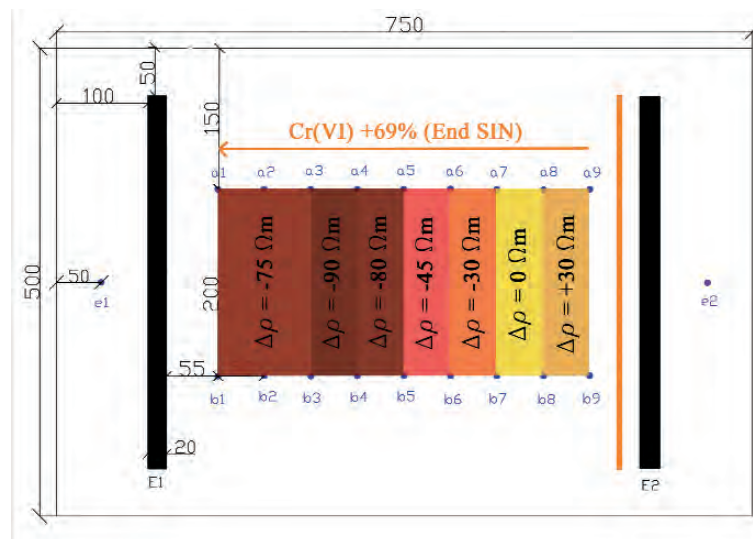| ID Sample	$\rho[\Omega m]$
Natural	99.93
Polluted	17.87
SA	48.84
SB	23.46
SC	16.73

Fig. 9 - Map of the electrical resistivity variations Δρ, highlighted by the colour, and Cr(VI) % flux from the starting orange line, near to the E2 electrode, to E1 electrode, between the start and the end of the SIN EKR linear process.

water-pollutant rested for 24 h, to reach the chemical equilibrium.

Three different EKR process time-chained were experimented. We used: a) DC voltage signal to control the natural period of the system; b) time-varying signal with a positive sinusoidal waveform; c) time-varying signal with inverted polarity and a positive sinusoidal waveform.

3.2. Experimental process and results

3.2.1. Process a: DC process

We used DC voltage for 68 h (Losito and Angelini, 2002), to find the period T [h] related to the charge/discharge cycle of the polluted sand; the period depends on polarization phenomena at quasi DC conditions and is specific of the sand-water-pollutant system (Losito and Angelini, 2002). This process allowed to define the voltage gradient to be applied to the time-varying EKR process (Losito and Angelini, 2002). The aim was to optimize the sinusoidal energizing signal, both as amplitude and period, for process b) and c) (Cherubini *et al*., 2002; Losito and Angelini, 2002; Hansen and Rojo, 2007; Ryu *et al*., 2010).

The experiment parameters of DC process were: i) V_{app}= 53 V for 40 h with the voltage gradient of 1 V/cm; ii) V_{app}= 31 V for 7 h and the voltage gradient of 0.7 V/cm; iii) V_{app}= 70 V for 21 h and, the voltage gradient of 1.4 V/cm (Cherubini *et al*., 2002; Reddy and Karri, 2006; Cang *et al*., 2009; Kim *et al*., 2009). From the monitored signals (Fig. 6) we can note that the electrical field was linear over the cell surface, and it took 3 h to reach the equilibrium, according to the local resistivity variations (Fig. 7): this behaviour show that the Cr(VI) diffusion process was reached as well confirmed by the chemical analysis (Table 3). The charge/discharge cycle was of 24 h (Fig. 6) as known in literature for different types of sands, but for the same pollutant (Cherubini *et al*., 2002; Losito and Angelini, 2002). The voltage gradient that produced the best
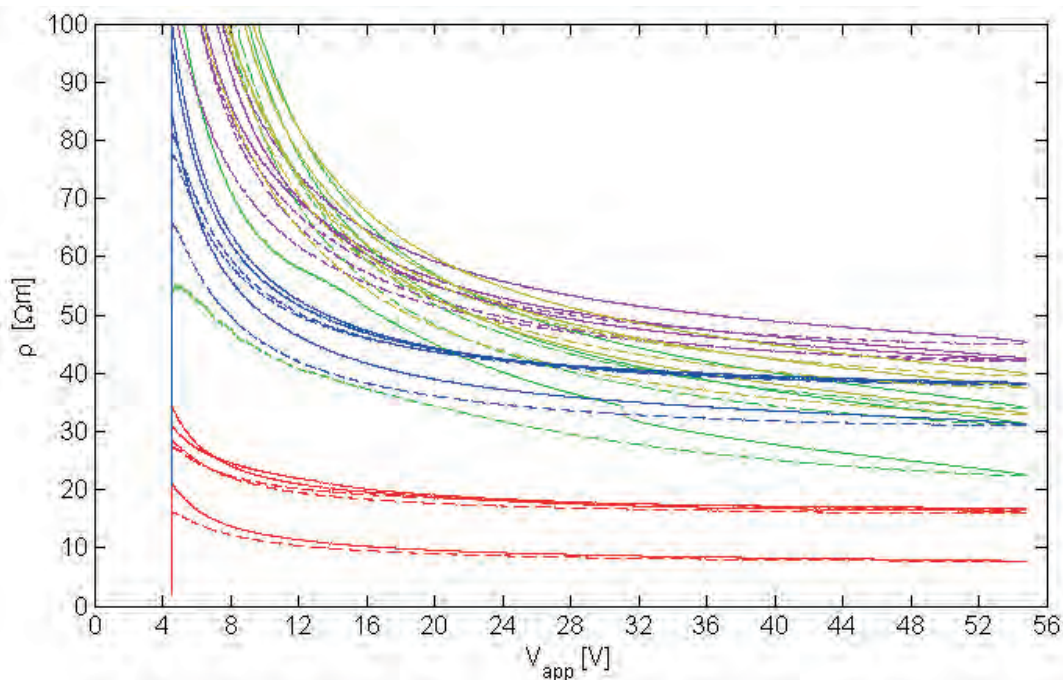
Fig. 10 - Electrical resistivity (ρi) versus the applied voltage (V_{app}) in the radial EKR sinusoidal process.; The solid lines indicate the positive voltage gradients (12 h), while the dashed lines the negative ones (12 h); the different colours indicate the distance i from the centre of the cell surface: red lines 3 cm, blue lines 13.5 cm, dark pink 24 cm, dark yellow 34.5 cm and green 42 cm.

ionic mobilization was 1 V/cm (Fig. 6), as already suggested from the literature (Cherubini *et al.*, 2002; Losito and Angelini, 2002).

Therefore, for process b) and c), we applied a positive sinusoidal waveform energizing signal with the voltage peak $V_p = 53$ V as amplitude and $T = 24$ h as period.

3.2.2. Process b: SIN process

We used a positive sinusoidal signal for 48 h. This process allowed to concentrate the highest pollutant content near the high voltage electrode (the "storage electrode") as confirmed by the time local resistivity evolution ($\rho_{12} = 15$ Ω·m, red lines in Fig. 8) and by the chemical analysis (Table 3).

3.2.3. Process c: SIN-INV process

We used the same positive sinusoidal energizing signal but with inverted polarity for 48 h. The local resistivity ρ_{12} (blue lines in Fig. 8) increases and shows a different trend, if compared with the SIN process: that means that the Cr(VI), which was stored near the E1 electrode (Fig. 9), moved to E2 electrode. The chemical analysis confirmed this process (Table 3).

Moreover, at the end of SIN EKR process the resistivity variations $\Delta\rho$ [Ω·m] (Fig. 9) and the chemical analysis (Table 3) showed that the DC-EKR process is less effective than the SIN-EKR process: this result was already obtained in previous experiments (Losito and Angelini, 2002;
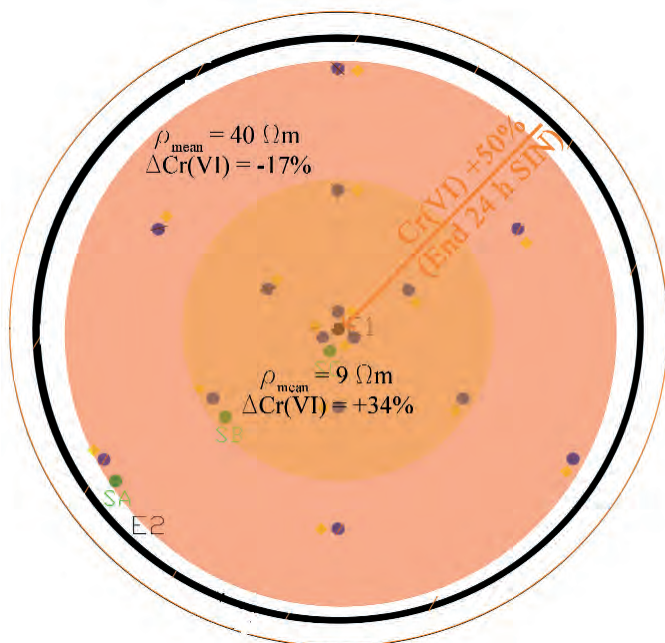
Fig. 11 - Map of the local mean electrical resistivity ρ_{mean} and of the mean Cr(VI) % content variations (orange: positive variations, light red: negative variations), produced by the sinusoidal EKR process. The orange arrow represent the Cr(VI) % flux from the E2 electrode, to E1 electrode.

Cherubini *et al*., 2002).

4. Radial electric field experiments

4.1. Experimental setup

The cylindrical cell ($\varnothing$ = 110 cm, h = 80 cm) was made of a non polarisable plastic material. It was filled 70 cm high with natural sand from Melfi (sand volume $\approx$ 665 dm^3) and then hydrated with tap water (50% as volume). A piezometer was used to control the saturation level. The sand granulometric and chemical-physical properties are shown in Tables 1 and 2.

The current electrodes were two carbon-nylon ropes ($\varnothing$ = 1 cm) by Pozzi Electa s.r.l. (Fig. 5b): the high voltage electrode was placed in the centre of the tank surface (E1 in Fig. 4b), while the circular low voltage electrode (3.5 m length, E2 in Fig. 4b) was placed 5 cm away from the tank wall. Both the electrodes were located 2 cm depth and were connected to electric circuit by two unipolar cables (Figs. 4a and 5c). For safety reasons, the electrodes, that stood out the ground, were inserted into an insulating pipe. Since some technical problems occurred (the high voltage electrode broke two times after 6 h of process), we decided to test the radial electric field using a stainless steel electrode as high voltage. This experiment worked only 24 h, to avoid the well-known redox problem on stainless steel (Cherubini *et al*., 2002).

Thirty voltage electrodes were placed on the sand surface to monitor the voltage during the process: fifteen were stainless steel electrodes ($\varnothing$ = 0.2 cm, L = 5 cm, 1 cm depth) and fifteen were non-polarisable electrodes (PMS 9000: Pb-PbCl$_2$ NaCl, $\varnothing$ = 3.2 cm, h = 18 cm). The electrodes were arranged in pairs (one for each type), according to six radial directions (e1-e15 in Fig. 4b). Each
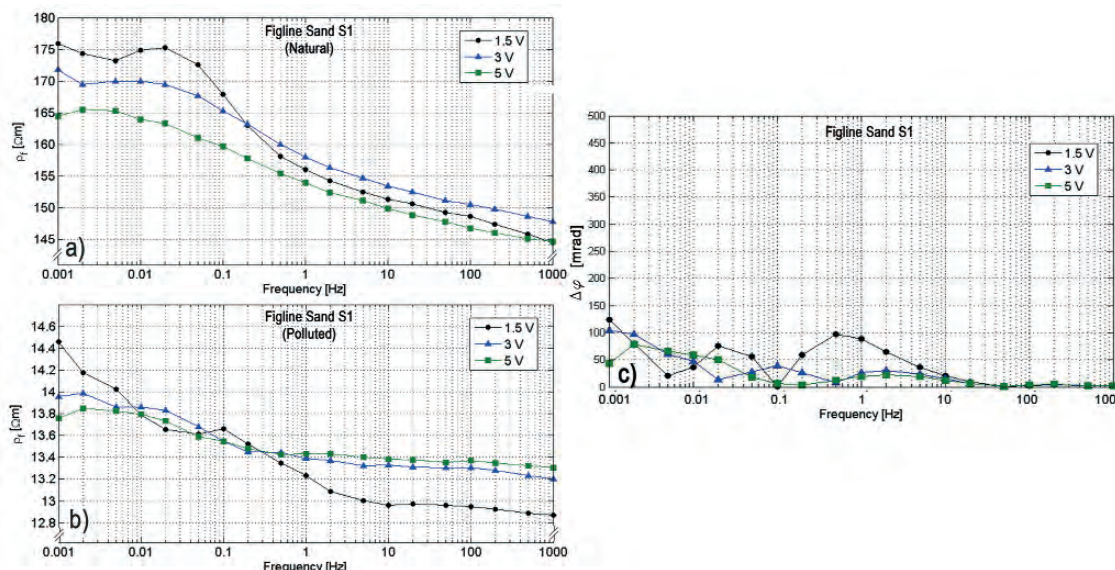
Fig. 12 - a) and b) Complex electrical resistivity ρ_f and c) difference $\Delta\phi$ between the phase displacement of the natural sample and the phase displacement of the polluted sample, versus frequency (0.001-1000 Hz) at three different maximum applied voltage (V_p = 1.5 V, 3 V and 5 V) of saturated Figline sand: sample S1 is natural and sample S1p is polluted with 4.4 g Cr(VI)/kg$_{dry\ soil}$.

electrode family was connected to the suitable data logger. We polluted the sand with 6 dm^3 of a 28.4 g Cr(VI) solution and poured it on the surface of the tank. The system rested for 24 h, so that the final polluted volume was about 20 dm^3. During this stand-by, the current electrodes were short-circuited to reach the electrical equilibrium of the system.

4.2. Experimental process and results

The radial electric field experiment was carried out to: a) know the efficiency of the radial electric field in EKR process; b) optimize this array (Kim *et al.*, 2005; Turer and Genc, 2005); c) validate the mechanical resistance of the rope electrode; d) compare the voltages obtained by using the stainless steel with the voltages obtained by using the non-polarisable electrodes.

For these purposes, we planned to apply a 24 h positive sinusoidal energizing signal (V_p = 64 V).

Since the rope in the centre of the tank broke down two times after 6 h of energization, we decided to use stainless steel material ($\varnothing$ = 1 cm, L = 20 cm) as high voltage electrode.

Concerning the two voltage electrode families, we observed that their response was quite similar, but the voltage of the impolarizable ones resulted about 2 V lower. To calculate the resistivity, we selected the signals obtained using the stainless-steel electrodes, thinking that the local voltage could have been modified by the electro-chemistry of the impolarizable electrodes.

The resistivity versus the applied voltage decreases during the first 12 h (half SIN wave signals), but increases during the following 12 h (second half of the SIN wave signal) (Fig. 10). This resistivity behaviour let us presume that a positive ramp up signal, with 12 h as period, should be more effective than the positive sinusoidal one, that is composed by a 12 h positive gradient, followed by a 12 h negative gradient.
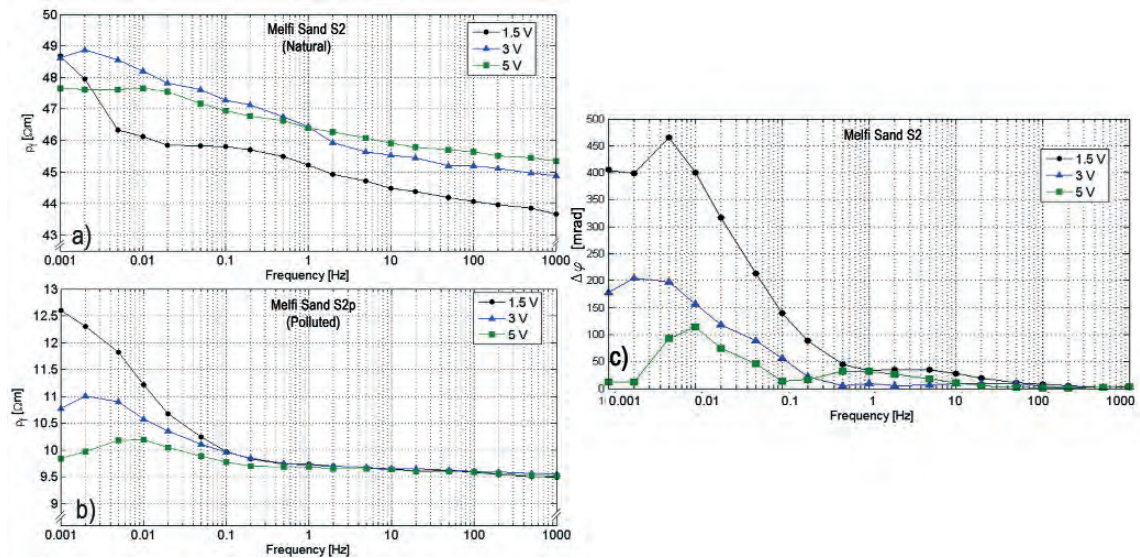
Fig. 13 - a) and b) Complex electrical resistivity ρ_f and c) difference $\Delta\phi$ between the phase displacement of the natural sample and the phase displacement of the polluted sample, versus frequency (0.001-1000 Hz) at three different applied voltages (V_p = 1.5 V, 3 V and 5 V) of saturated Melfi sand: sample S2 is natural and sample S2p is polluted with 400 mgCr(VI)/kg$_{dry\ soil}$.

On the basis of both the mean local resistivity and the Cr(VI) variations (Fig. 11), the final EKR effects produced by a radial electric field resulted lower respect to those of all the experiments made using a linear electrical field.

5. Sample electrical parameters for the local resistivity calibration

5.1. Experimental setup

To calibrate the local resistivity variation occurred during the EKR processes, we calculated also the complex resistivity, the phase displacement φ [mrad], and the phase displacement difference $\Delta\varphi$ between the natural and polluted sample using only the fundamental frequency of the all signals, of seven selected samples, employing the quadripole technique (Losito *et al*., 2001). The sample holders were PVC cylinders ($\varnothing$ = 3.5 cm, L = 10.5 cm); the current electrodes were two stainless steel plates ($\varnothing$ = 3.5 cm, h = 0.5 cm) and the voltage electrodes were a grid of a Ni-Cr wire ($\varnothing$ = 0.03 cm).

The selected samples were: sand from Figline, natural (S1), and polluted (S1p) with 4.4 g Cr(VI)/kg$_{dry\_soil}$; sand from Melfi, natural (S2) and polluted (S2p) with 400 mg Cr(VI)/ kg$_{dry\_soil}$; cylindrical cell logged samples (SA, SB, SC), respectively with 500.2 mg Cr$_{tot}$/ kg$_{dry\_soil}$, 792.1 mg Cr$_{tot}$/ kg$_{dry\_soil}$ and 483.3 mg Cr$_{tot}$/ kg$_{dry\_soil}$ content. These Cr$_{tot}$ content values were calculated by means of chemical analysis.

For each sample, the complex resistivity parameters were measured applying a sinusoidal waveform signal. We used three different peak voltage amplitudes (V_P = 1.5 V, V_P = 3 V; V_P = 5 V) and we took three measurements for each decade on the frequency interval 1 mHz-1 kHz (Losito and Angelini, 2002). In order to avoid strong electrical stresses, and consequently non-linear polarization
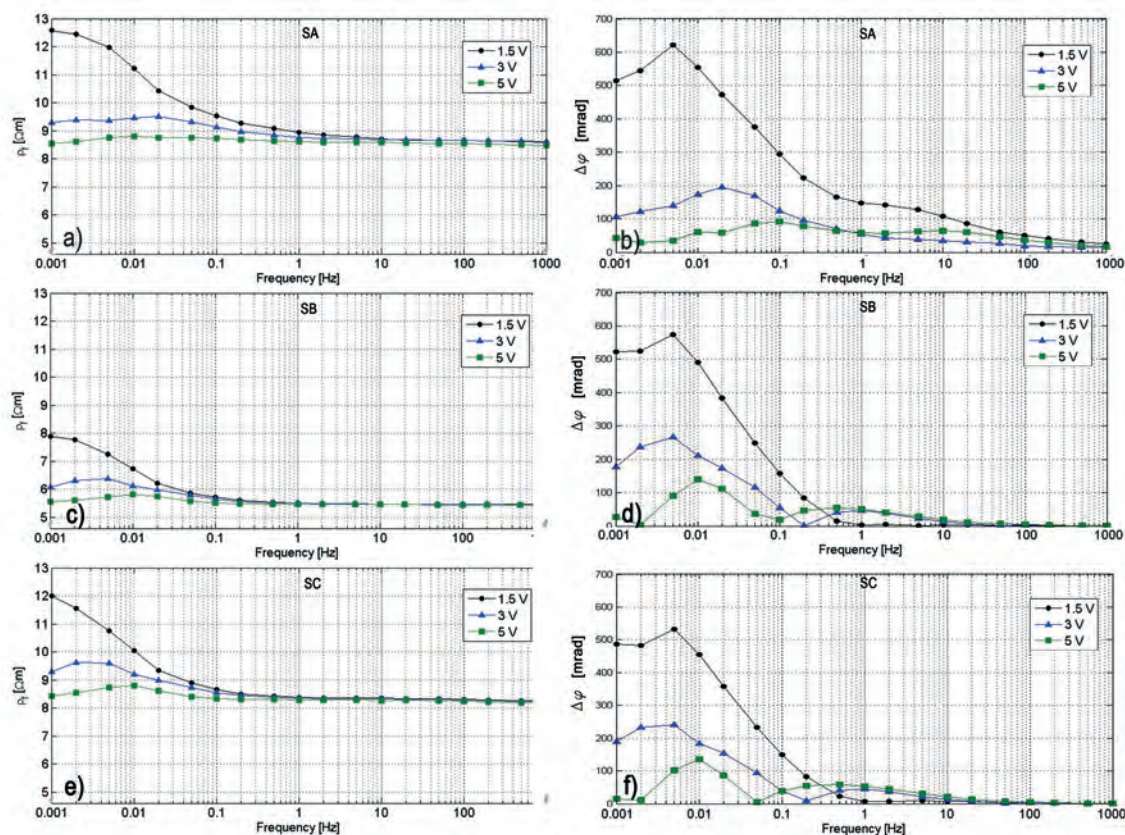
Fig. 14 - a), c) and e) Complex electrical resistivity ρ_f and b), d) and f) difference $\Delta\phi$ between the phase displacement of the natural sample (S2) and the phase displacement of the polluted sample (SA, SB and SC), versus frequency (0.001-1000 Hz) at three different maximum applied voltage (V_p = 1.5 V, 3 V and 5 V). The three logged samples (SA, SB and SC) were polluted, respectively, by 500.2 mgCr$_{tot}$/kg$_{dry\ soil}$, 792.1 mgCr$_{tot}$/kg$_{dry\ soil}$ and 483.3 mgCr$_{tot}$/kg$_{dry\ soil}$.

at quasi-DC conditions, we started from higher frequencies and lower voltage amplitude (Losito *et al.*, 1995, 1998; Losito and Angelini, 2002).

5.2. Results

The ρ_f of the natural sample (S1, S2) (Fig. 12a) confirmed the ρ_{DC} measured in the rectangular and circular cells, respectively before the sand pollution. In general the ρ_f of the samples are non-linear and depend on both the amplitude of the applied signal and the frequency ($f \leq 1$ Hz) mainly if the silt and clay components are relevant (Melfi sand) (Figs. 12a and 13a). The S1 and S2 $\Delta\phi$ confirms the presence of IP phenomena at very low-frequencies produced by the pollutant (Figs. 12c and 13c). This behaviour is strong if low voltages (V_p = 1.5 V) were applied to the sample (Melfi sand).

The different behaviour of the S1P and S2P complex resistivity (Figs. 12b and 13b), mainly using V_p = 1.5 V, on the whole frequency spectrum, could be due to the different chemical-physical properties of the two sands, and not to the different Cr (VI) content, because the silica component of

the Melfi sand is strongly higher than the silica content of the Figline sand.

The S1-S1p $\Delta\phi$ (Fig. 12c) has no relevant peaks, given the low silica content.

The S2-S2p $\Delta\phi$ at $V = 1.5$ V and $f < 0.1$ Hz (Fig. 13c) is related to the strong interaction between the CR(VI)content and the silt component of the sand.

The SA, SB, and SC complex resistivity trend (Figs. 14a, 14c and 14e) was comparable and strongly related to the Cr(VI) content, while the $\Delta\phi$ phase displacement (Figs. 14b, 14d, and 14f) was higher at $V_p = 1.5$ V and $f < 0.01$ Hz. We suppose that the $\Delta V = 0.125$ V/cm ($V_p = 1.5$ V) applied to the sample is the threshold voltage gradient, that actives the induced polarization phenomena. So we can state that the sinusoidal EKR process activated all the IP phenomena, that have been observed in sample electrical behaviour.

In addition, we also calculated the complex resistivity at very high frequency ($f \approx 15$ kHz) of the S2, S2p, SA, SB and SC samples using the two-pole technique, by a Wayne Kerr precision component analyser. The results are showed in Table 4 and are in agreement with the cylindrical cell resistivity (Fig. 10) and with the complex resistivity calculated in the frequency range of 1 mHz – 1 kHz (Figs. 14a, 14c, and 14e).

In general, the sample electrical resistivity behaviour resulted non linear mainly at low frequencies and the pollutant increased the non linear behaviour. At very low frequencies the THD% parameter (Losito *et al*., 1995) was 30% for Melfi polluted samples ($V_p = 1.5$ V): this high non linearity indicates the activation of fluid/solid interactions that cannot be described by classical models.

6. Conclusions

In this paper we presented the results of recent EKR experiments at laboratory scale, carried out to evaluate the effects of the linear and the radial electric field on the EKR efficiency in soils polluted by heavy metals. The experimental method, previously defined from the authors, is based on the enhancement of EKR process in fine-grained and/or clayey soils. This enhancement is related to the electrical behaviour of polluted soils, that is strongly non-linear at very low frequencies ($f < 0.01$ Hz) and is specific of hydrated silicates; the hydro-silica layers allow to move the heavy metals, if we apply to the soil an electrical field that is positive, sinusoidal, and with $T > 100$ s. Previous EKR experiments, carried out at DC conditions, suggested an energizing period of 24 h.

In the experiments of this paper we used sand polluted by the Cr(VI), that has been selected as heavy metal.

To evaluate the efficiency of the EKR processes, we made the chemical analysis, measured the complex resistivity of sand samples logged from the experimental cells, and we monitored simultaneously the applied voltage V_{app}, the current I and the local electric field on the sand surface. These electrical signals allowed to evaluate, versus time, the local electrical resistivity ρ_{ij}. The ρ_{ij}, calibrated by using the sample ρ_f and chemical analysis, resulted a suitable parameter of the metal flux, produced by the EKR action.

The interpretation of the EKR process has been accomplished by the ρ_f behaviour of the natural and Cr(VI) polluted samples, that confirmed the existence of non linear electrical polarizations at very low frequencies and consequently the possibility of hydro-silica metal transport. The non linear behaviour produced very high values of the THD% parameter (up to 30%) in polluted Melfi sand and displacement phase differences $\Delta\phi$ between the natural and the

polluted Melfi sand up to 650 mrad at very low frequencies ($f \leq 0.1$ Hz).

The joint evaluation of all the selected parameters allowed to conclude that the main experiment result is that, despite the lacking of the silt and clay components in the used sand, the linear-EKR process moved the 69% of Cr(VI) after the sinusoidal process. In fact, the radial-EKR process, carried out with a very fine silica sand, moved only the 34% of Cr(VI) after the sinusoidal process.

Starting from electrical parameters, both of cells and samples, and results of the chemical analysis, we can deduce that the EKR process not only moved the Cr(VI) to the high voltage electrode, but also electrodeposited it on the electrode itself. This hypothesis, confirmed by recent experiments, allows us to say that the linear-EKR is more effective than the radial-EKR because the "storage surface electrode" is greater.

Moreover, the electrical resistivity versus voltage was unstable at low voltage: it seemed to be influenced by the negative gradient of the sinusoidal signal. This phenomenon is enhanced by the resistivity decrease produced during the SIN-INV EKR process with linear electrodes.

We presumed that a positive ramp up signal, with a period of 12 h, should be more effective than the positive sinusoidal one. This result make it possible to resolve many technical instrumental problems, and so to reduce the EKR costs. The recent results of the experiments carried out with a ramp up signal confirmed this hypothesis.

REFERENCES

Acar Y.B. and Alshawabkeh A.N.; 1993: *Principles of electrokinetic remediation.* Environ. Technol., **27**, 2638-2647.

Baraud F., Tellier S. and Astruc M.; 1997: *Ion velocity in soil solution during electrokinetic remediation.* J. Hazard. Mater., **56**, 315-332.

Cang L., Zhou D-M., Wang Q-Y. and Wu D-Y.; 2009: *Effects of electrokinetic treatment of heavy metal contaminated soil on soil enzyme activities.* J. Hazard. Mater., **172**, 1602-1607.

Cherubini F., Losito G., Trova A. and Angelini R.; 2002: *Signal optimization for electrokinetic metal decontamination: sample and field scale model experiments.* In: Proc. 8th meeting EEGS, Aveiro, Portugal, Extended Abstract, pp. 211-214.

Hamed J., Acar Y.B. and Galer J.; 1991: *Pb(II) removal from kaolin by electrokinetics.* J. Geotech. Eng., **117**, 241-271.

Hansen H.K. and Rojo A.; 2007: *Testing pulsed electric fields in electroremediation of copper mine tailings.* Electrochim. Acta, **52**, 3399-3405.

Kim W.S., Kim S.O. and Kim K.W.; 2005: *Enhanced electrokinetic extraction of heavy metals from soils assisted by ion exchange membranes.* J. Hazard. Mater., **118**, 93-102.

Kim D.H., Ryu B.G., Park S.W., Seo C.I. and Baek K.; 2009: *Electrokinetic remediation of Zn and Ni-contaminated soil.* J. Hazard. Mater., **165**, 501-505.

Losito G. and Angelini R.; 2002: *Physical parameters activating electrical signal distortions in polluted soils.* Ann. Geophys., **45**, 207-217.

Losito G. and Finzi-Contini G.; 1981: *Laboratory instrumentation to study changes of electrical conductivity of rocks with*

changes of frequency, temperature and pressure. Geophys. Prospect., **29**, 923-931.

Losito G., Muschietti M. and Trova A.; 1991: *Laboratory electrical responses of rock samples under geothermal temperature-hydrostatic pressure conditions.* Geothermics, **20**, 165-178.

Losito G., Muschietti M. and Trova A.; 1995: *Electrical effects of pollutants in earth soils and sedimentary rocks.* In: Proc. 1st meeting EEGS, Torino, Italy, Extended Abstract, pp. 57-60.

Losito G., Schnegg P.A., Lambelet C., Viti C. and Trova A.; 2001: *Microscopic scale conductivity as explanation of magnetotelluric results from the Alps of the Western Switzerland.* Geophys. J. Int., **147**, 602-609.

Losito G., Trova A. and D'Urso I.; 1998: *Frequency and DC electrical behaviour of polluted sediments in industrial areas: field and laboratory investigations.* In: Proc. 4th meeting EEGS, Barcelona, Spain, Extended Abstract, pp. 35-38.

Olhoeft G.R.; 1979: *Nonlinear electrical properties.* In: Neel L. (ed), Nonlinear behaviour of molecules, atoms and ions in electric, magnetic and electromagnetic fields. Elsevier, pp. 395-409.

Parasnis D.S.; 1965: *Theory and practice of electric potential and resistivity prospecting using linear current electrodes.* Geoexploration, **3**, 3-69.

Reddy K.R. and Chinthamreddy S.; 1999: *Electrokinetic remediation of heavy metal-contaminated soil under reducing environments.* Waste Management, **19**, 269-282.

Reddy K.R. and Karri M.R.; 2006: *Effect of voltage gradient on integrated electrochemical remediation of contaminant mixtures.* Land Contam. Reclam., **14**, 685-698.

Reddy K.R., Xu C.Y. and Chinthamreddy S.; 2001: *Assessment of electrokinetic removal of heavy metals from soils by sequential extraction analysis.* J. Hazard. Mater., **84**, 279-296.

Ryu B-G., Yang J-S., Kim D-H. and Back K.; 2010: *Pulsed electrokinetic removal of Cd and Zn from fine-grained soil.* J. Appl. Electrochem., **40**, 1039-1047.

Telford W.M., Geldart L.P., Sheriff R.E. and Keys D.A.; 1976: *Applied Geophysics.* Cambridge University Press, Cambridge, U.K., 860 pp.

Turer D. and Genc A.; 2005: *Assessing effect of electrode configuration on the afficiency of electrokinetic remediation by sequential extraction analysis.* J. Hazard. Mater., **119**, 167-174.

US Army Environmental Center; 2000: *Final Report – In situ electrokinetic remediation of metal contaminated soil, technology status report.* Report Number: SFIM-AEC-ET-CR-99022, 30 pp.

Virkutyte J., Sillanpää M. and Latostenmaa P.; 2002: *Electrokinetic soil remediation: a critical overview.* Sci. Total Environ., **289**, 97-121.

Zhang P., Jin C., Zhao Z. and Tian G.; 2010: *2D crossed electric field for electrokinetic remediation of chromium contaminated soil.* J. Hazard. Mater., **177**, 1126-1133.

Corresponding author: Gabriella M.S. Losito
                          DICeA, Università di Firenze
                          Via di Santa Marta 3, 50139 Firenze, Italy
                          Phone: +39 055 4796323; fax: +39 055 495333; e-mail: losito@dicea.unifi.it